JOURNAL OF MATERIALS SCIENCE 20 (1985) 1434–1444

Rubber toughening of plastics

Part 8 *Effects of glass beads on the kinetics of creep in ABS*

CLIVE B. BUCKNALL, S. ERIC REDDOCK*
School of Industrial Science, Cranfield Institute of Technology, Cranfield, Bedford, UK

Creep measurements were made on a series of six ABS blends containing 0 to 20 vol % of 80 μm glass beads. At small strains, the beads raised the modulus of the ABS. However, debonding of the polymer from the glass resulted in a rapid drop in modulus with increasing strain ϵ and bead content ϕ, and at strains above 1.0% the order of stiffnesses was reversed. Debonding resulted in an increase in creep rate with ϕ, as measured by the time τ to reach 1% volume strain. Plots of ln τ^{-1} against applied stress σ were linear, in accordance with the Eyring equation, and provided data for comparing stress concentration factors γ. The relationship between γ and ϕ fitted approximately to the Ishai–Cohen effective area model. It is concluded that debonded glass beads accelerate multiple crazing by increasing average stresses in the ABS matrix, and in that respect resemble rubber particles. However, unlike rubber particles, debonded beads drastically reduce notched Charpy impact strength.

1. Introduction

Rigid particulate fillers are added to plastics both to improve properties and to reduce costs. However, improvements in properties are usually restricted to increases in stiffness and reductions in coefficients of expansion, and are often accompanied by reductions in fracture resistance. These effects are in marked contrast to those produced by spherical rubber particles, which lower modulus and greatly increase fracture toughness. Nevertheless, there are some similarities between the two types of composite. Spherical glass beads, like rubber particles, initiate crazing in styrene–acrylonitrile (SAN) copolymer under tension, causing the composite to yield at a stress well below the failure stress of the SAN [1]. Extensions to break, on the other hand, are very different in the two cases: glass-filled SAN, having yielded, fails at a strain below 3%, whereas rubber modified SAN (ABS polymer) reaches strains of 20% or more. In examining glass-filled ABS, the present paper considers both types of spherical particle, highlighting similarities and differences. The use of tough ABS rather than the relatively brittle SAN as a matrix offers greater scope for experiments on yield and fracture behaviour of glass-filled polymers.

2. Experimental procedure

2.1. Materials

A single batch of Lustran 740 ABS manufactured by Monsanto was used for all experiments. The polymer was blended with Ballotini 2024 glass microspheres ranging in diameter from 25 to 150 μm, with a mean of 80 μm, and an approximately normal size distribution. The beads consisted of soda A glass, and were coated with a silane coupling agent suitable for polypropylene. Blends were made in a small laboratory internal mixer running at a temperature of 148° C, with a mixing time of 3 min. The hot blends were then converted to thin sheet on a two roll mill, cooled, and granulated.

The granules were compression moulded at 190° C into sheets measuring approximately 6.4 mm x 250 mm x 250 mm. The sheets were

Present address: British Aerospace, Argyle Way, Stevenage, Herts, UK.

0022–2461/85 $03.00 + .12

subsequently annealed under vacuum by placing them in an oven preheated to 120° C, which was switched off after an hour, allowing the material to cool to room temperature over a period of 7 h. The densities of the blends were measured in a density bottle in order to check the concentrations of glass beads. Calculated volume fractions, ϕ, were 0, 0.01, 0.045, 0.102, 0.149 and 0.204.

2.2. Testing

Specimens for mechanical testing were machined from the compression moulded sheet. As in previous studies [2–5], creep measurements were made on dumb-bell specimens with a parallel gauge portion 40 mm long and 5 mm wide, in a room controlled at 20 ± 0.5° C and 65% RH. Tensile stresses were applied by lever loading, and the resulting longitudinal and lateral strains were measured simultaneously using high accuracy extensometers. Each long-term test was preceded by a loading–unloading programme at successively increasing loads, in order to obtain a 100 sec isochronous curve of tensile creep modulus against 100 sec longitudinal strain within the low strain region. During this preliminary programme, stresses were kept well below those used for long-term testing.

Tensile tests at constant strain rate were carried out at 23° C on ASTM Type 1 specimens, using a Nene tensometer operating at a crosshead speed of 5 mm min^{-1}. The same crosshead speed was used for flexural tests on notched rectangular bars, which measured 6.4 mm × 12 mm × 150 mm, with a single central edge notch cut to a depth of 0.64 mm into the broader face of the bar. The notch was machined with a sharp rotary cutter giving a total tip angle of 22.5°. The bars were loaded in three-point bending, using a span of 100 mm. Rectangular bars for Charpy impact testing measured 6.4 mm × 12 mm × 57 mm. The same cutter was used to notch the specimens, but the notch was cut into the narrower face of the bars, to a depth of 0.90 mm. Impact tests were carried out at 23° C using a Zwick pendulum machine with a specimen span of 40 mm. Fracture surfaces were coated with gold/palladium and examined by scanning electron microscopy.

3. Results

The relationship between Young's modulus, E, and tensile strain, e_3, after 100 sec under load is shown in Fig. 1, which includes data obtained both from the preliminary loading–unloading tests and from the early stages of long-term tests. At strains below 0.1% the glass beads increase modulus as expected. Above 0.1% extension, however, the modulus begins to show a dependence upon strain that is especially marked in blends containing a higher concentration of beads. At strains above 1%, the order of stiffnesses has become reversed, with the unfilled ABS having the highest creep modulus. This point is further emphasized in Fig. 2, which shows the relationship between modulus and volume fraction of beads at several different strains. It is clear that debonding of the glass from the ABS begins at strains of 0.25% or less.

Typical creep curves for the unfilled ABS and for a blend containing 20.4 vol% glass beads, are presented in Figs. 3 and 4. The behaviour of the unfilled polymer is similar to that observed previously in ABS [3]: the volume strain, ΔV, changes very slowly during the initial stages of the test, but rises rapidly after 3000 sec under load, whereas the negative area strain, $-\Delta A$, increases relatively slowly throughout the test. The extension e_3, is equal to $(\Delta V - \Delta A)$ when strains are small, so that the two curves represent the respective contributions of dilatation and shear deformation to the total strain [6]. The kinetics of creep in the filled ABS are distinctly different from those in the unfilled ABS: in the filled material ΔV increases at an almost constant rate throughout the test. Detailed examination of the data shows that the rate is highest immediately after loading, and becomes slower with time. Again, the time-dependent change in area is relatively small. The major contribution to time-dependent deformation is dilatation, which in this case includes not only crazing in the ABS matrix, but also cavitation resulting from debonding of the glass beads.

The change in kinetics from a rapidly increasing rate of dilation in unfilled ABS to a slightly decreasing rate in the blend containing 20 vol% beads occurs progressively with increasing glass content. A significant flattening of the curve is already apparent at 1 vol% filler. For any given material, raising the applied stress, σ, causes an increase in creep rate, but does not significantly alter the shape of the creep curve. At any given stress, the creep rate increases with volume fraction, ϕ, of glass beads.

The time taken for the material to reach a volume strain of 1.0% is indicated in Figs. 3 and 4.

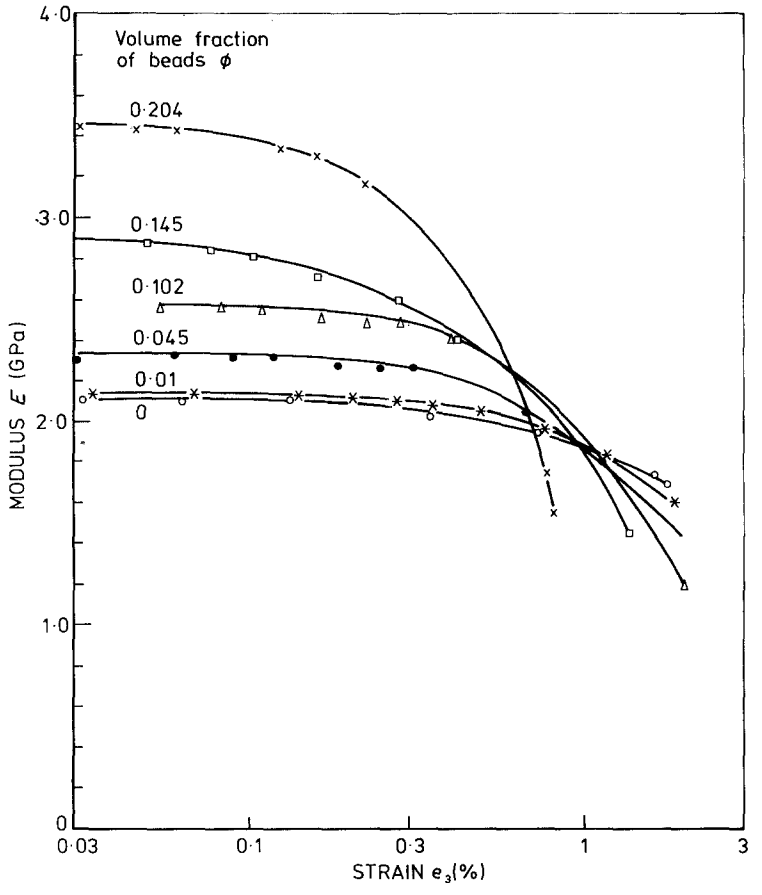

Figure 1 Isochronous curves of 100 sec creep modulus against 100 sec extension for blends of ABS with glass beads.

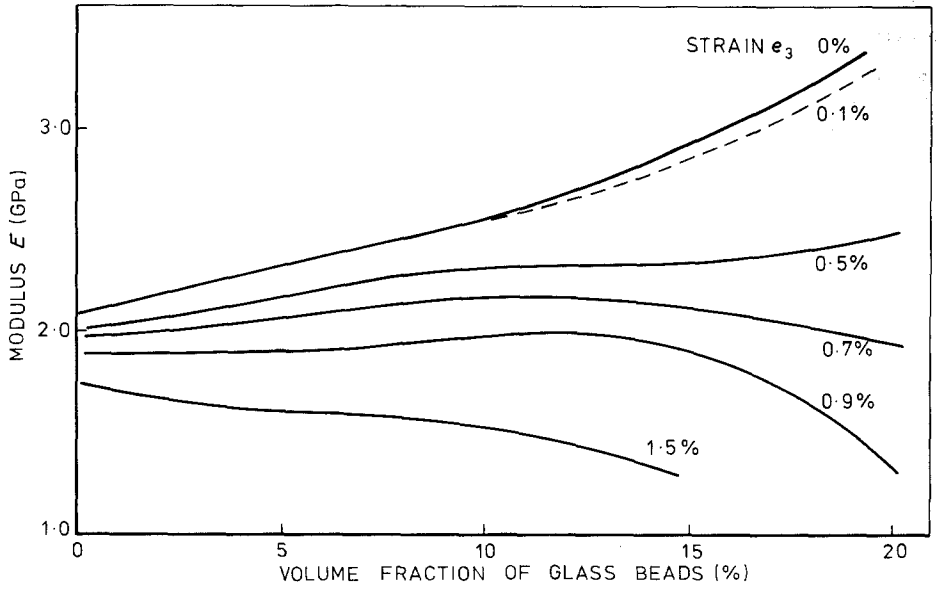

Figure 2 Data from Fig. 1 replotted to show the relationship between 100 sec modulus and bead content at various 100 sec strains.

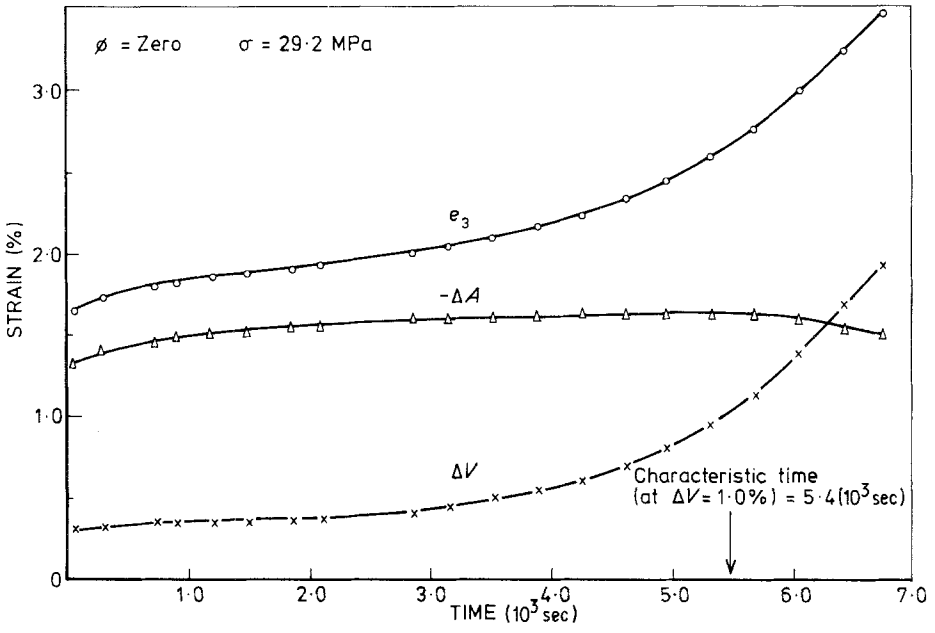

Figure 3 Creep curves for unfilled ABS.

This "characteristic time", τ, is a simple measure of the creep rate, which avoids the problem of writing a kinetic equation (relating strain to time through a rate coefficient, κ) for each material. A more detailed treatment of κ in specific cases is given in previous publications [4–6]. Since creep and other rheological processes are activated, the effects of stress and temperature can be correlated through the Eyring equation:

$$\kappa = 2Q \sinh(\gamma V^* \sigma / kT) \simeq Q \exp(\gamma V^* \sigma / kT) \quad (1)$$

where Q is a constant at any temperature T, k is Boltzmann's constant, V^* is activation volume, and γ is a stress concentration factor, defined as the local stress at the site of flow divided by the applied stress, σ. Values of γ for particulate

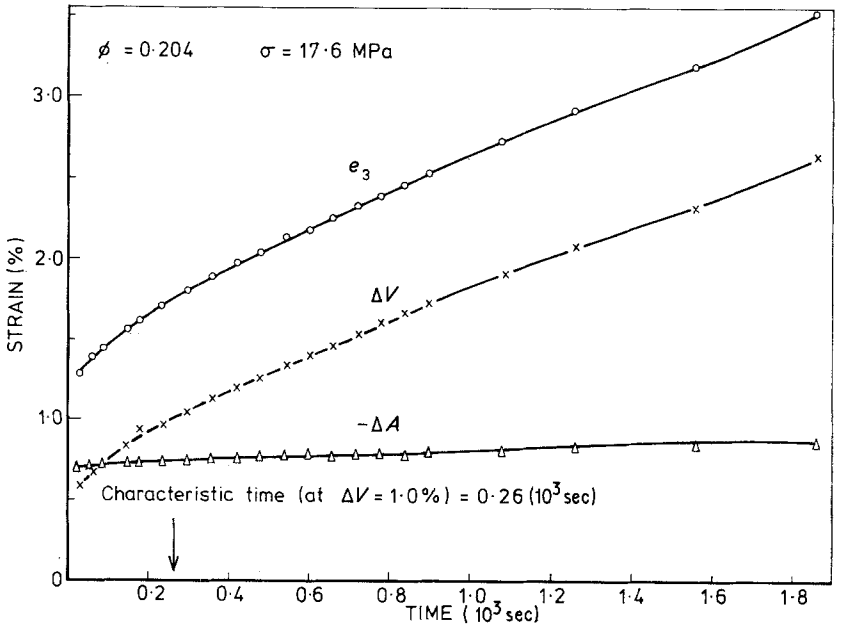

Figure 4 Creep curves for ABS containing 20.4 vol% glass beads.

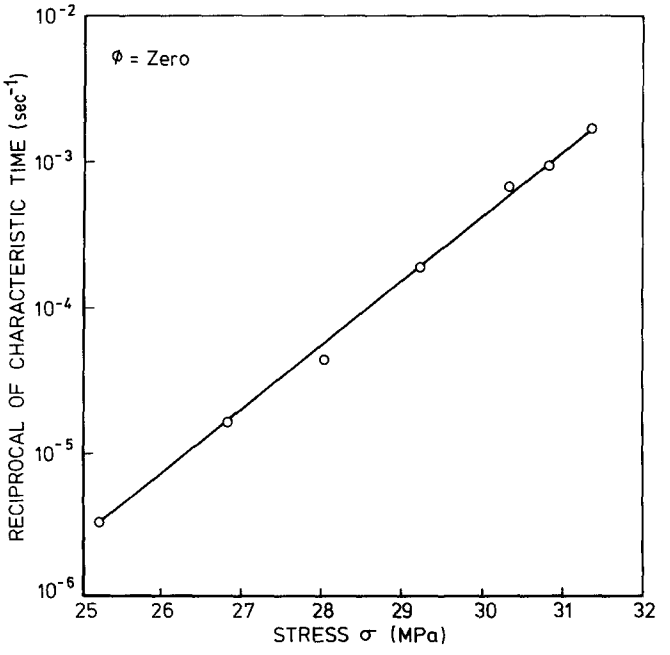

Figure 5 Eyring plot for unfilled ABS.

composites based on a single matrix polymer can be compared by plotting log κ against σ at constant temperature, provided that V^* does not change with composition. If, as in the present case, the strain rate is a function of strain, a similar analysis can be made by plotting log τ^{-1} against σ, since

$$de/dt = \kappa f(e) \quad (2)$$

which on integration, irrespective of the form of $f(e)$, gives:

$$\kappa\tau = \text{constant} \quad (3)$$

Figs. 5 and 6 show Eyring plots for blends containing 0% and 20% glass beads. Both materials give a linear relationship, but with different slopes. If the same mechanism controls the rate of deformation in both materials, so that V^* remains unchanged, this observation means that γ is increased on addition of glass beads – a not unexpected conclusion. Results for the whole series of blends are presented in Fig. 7, which shows that γ increases systematically with ϕ. Fig. 8 is a master curve obtained by plotting log τ^{-1} against $\sigma\gamma/\gamma_0$, where γ/γ_0 is the ratio of slopes for filled and unfilled ABS calculated from the Eyring data in Fig. 7. The value of γ_0 will, of course, depend upon the concentration of rubber particles in the ABS, and is therefore not assigned a value of unity in this treatment.

Fig. 9 shows the relationship between the glass concentration, ϕ, and γ/γ_0, which can be regarded as the stress concentration factor due to the addition of the beads. The experimental data are compared with the predictions of the effective area model proposed by Ishai and Cohen [7]:

$$\gamma = [1 - \pi(3\phi/4\pi)^{2/3}]^{-1} \quad (4)$$

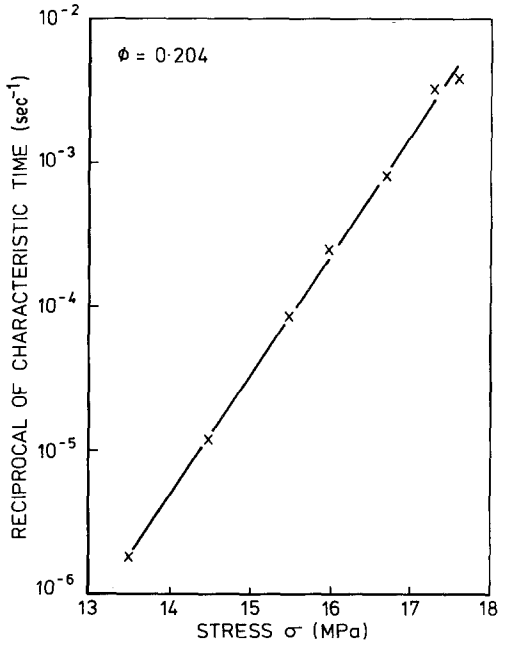

Figure 6 Eyring plot for ABS containing 20.4 vol% glass beads.

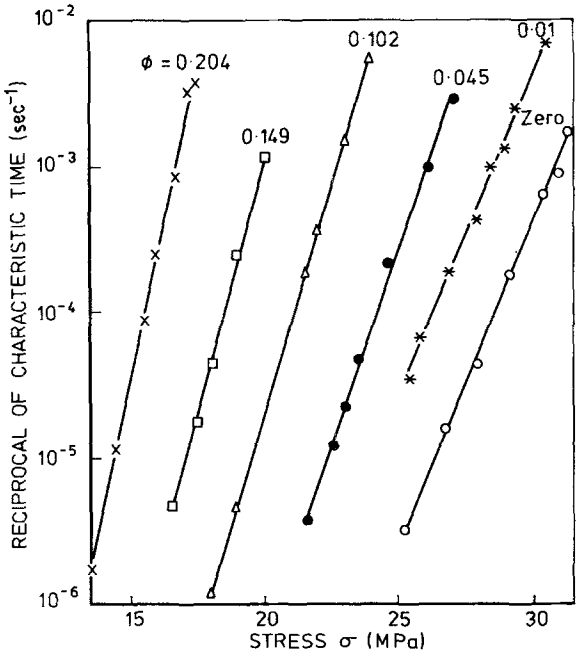

Figure 7 Eyring plots for the six ABS compounds.

The contributions of dilation and shear deformation to overall extension can conveniently be compared by plotting volume strain against elongation, as in Figs. 10 and 11. The results for the unfilled polymer are similar to those reported previously for ABS [3]: shear deformation is present throughout each test, but crazing and other dilation processes make an increasingly large contribution as the test proceeds, becoming more dominant as the applied stress is increased. Addition of only 1 vol% glass beads is sufficient to reduce substantially the strain at which dilation becomes the dominant deformation mechanism, and further additions move the curve further to the left; at 20 vol% the slope of the line is 0.95.

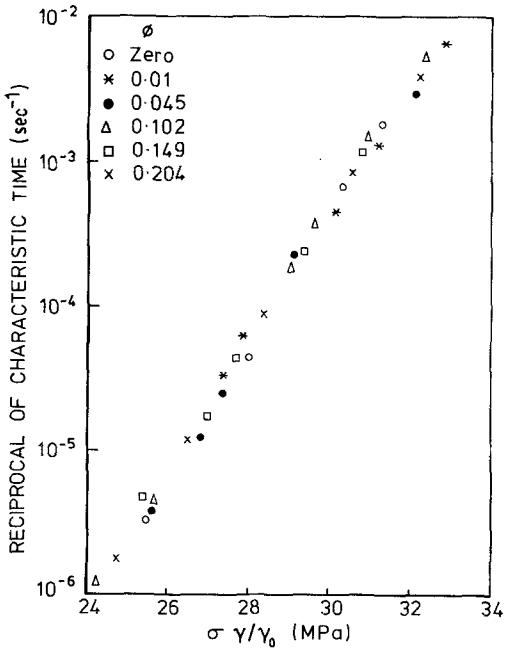

Figure 8 Eyring master curve of data from Fig. 7.

The effects observed in creep are reflected in the tensile test results. In the unfilled ABS, there is an increase in strain rate during creep at constant stress, and a corresponding decrease in stress immediately after the yield point during tensile testing at constant strain rate. At high filler loadings the creep strain rate is almost constant, and correspondingly there is no load drop following yield. The yield stress, σ_y, decreases with ϕ as illustrated in Fig. 12, the values at higher bead contents falling below those predicted by Equation 4. Fracture resistance drops rapidly on addition of glass beads to the ABS. Results from the sharp-notch Charpy test are given in Fig. 13; a similar curve was obtained from the slow three-point bend tests. Force–deflection curves for filled and unfilled ABS show that the reduced energy to break of the filled materials involves a reduction in both force and deflection at the load maximum.

Scanning electron microscopy of the fracture surfaces confirms that the beads become completely debonded, and shows that the resulting

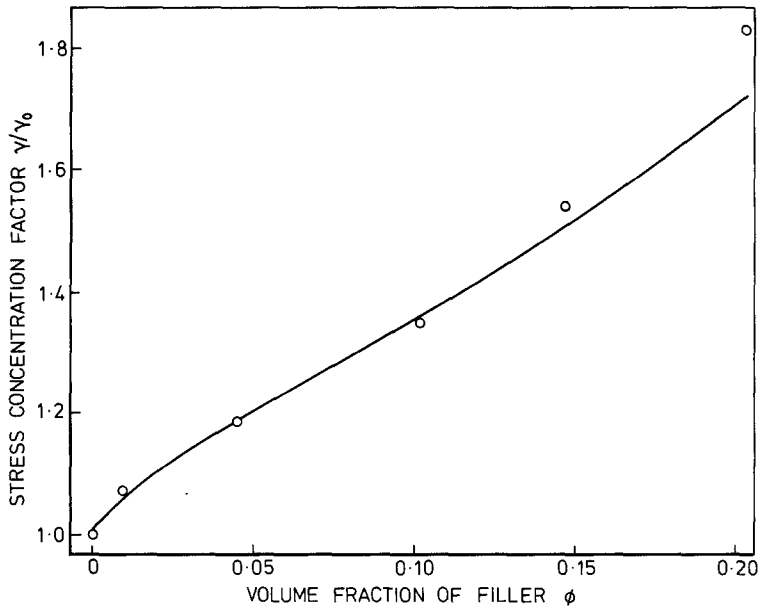

Figure 9 Relationship between Eyring stress concentration factor and volume fraction of glass beads. Solid line shows Ishai–Cohen curve.

spherical cavity expands as the deformation proceeds. Fig. 14 illustrates these points. There is no sign of adhesion between the glass microspheres and the ABS matrix, and a comparison between the remaining spheres and the associated cavities on the fracture surface indicates the extent of ductile deformation in the ABS.

4. Discussion

There is little evidence in this work of any significant adhesion between the glass beads and the matrix; nor would any be expected in view of the choice of silane coating for the glass. Hoop stresses developed in the ABS as a result of differential contraction on cooling from the glass transition are sufficient to ensure contact with the beads at small strains, but debonding begins at an early stage, and appears to be complete at strains of less than 2.0%. As a result of debonding, the blends behave essentially like foams containing 1 to 20 vol% of well dispersed spherical voids.

Stress concentrations in the ABS surrounding the debonded beads account for the increased creep rates and reduced yield stresses in the

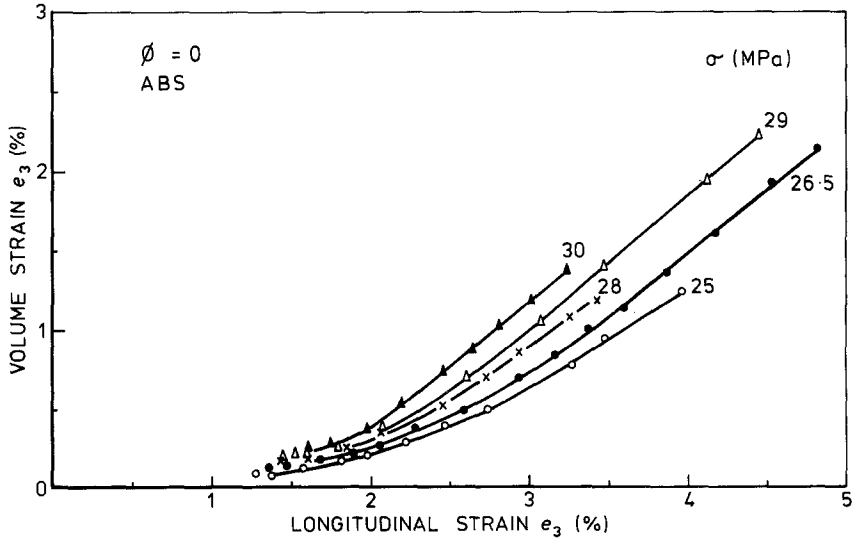

Figure 10 Relationship between volume strain and extension over a range of applied stresses for unfilled ABS.

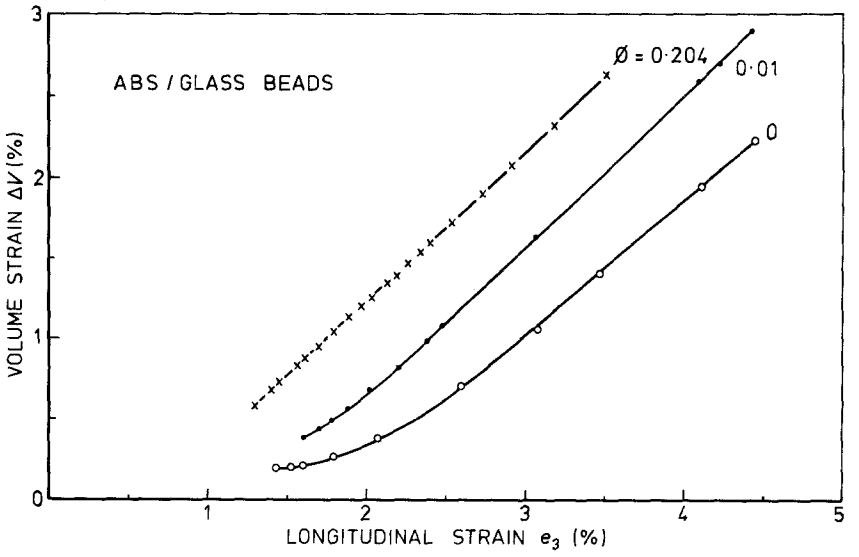

Figure 11 Relationship between volume strain and extension in creep tests on: (○) unfilled ABS at 29 MPa; (●) 1 vol% beads at 28.9 MPa; and (X) 20.4 vol% beads at 17.6 MPa.

composites. Creep and yield involve a complex series of processes, including initiation and propagation of crazes and shear zones in the ABS, and expansion of the spherical cavities formed around the glass beads. In each sequence of events there is a rate controlling step – a concept that is familar to the physical chemist – and it is the influence of stress concentrations upon this rate-controlling step that governs the relationship between the rate coefficient and the applied stress. Deformations occur most rapidly in regions of maximum stress concentration, close to the equators of voids or rubber particles. However, the most rapid stage of deformation would not be expected to be rate limiting: regions of lower stress concentration, through which the

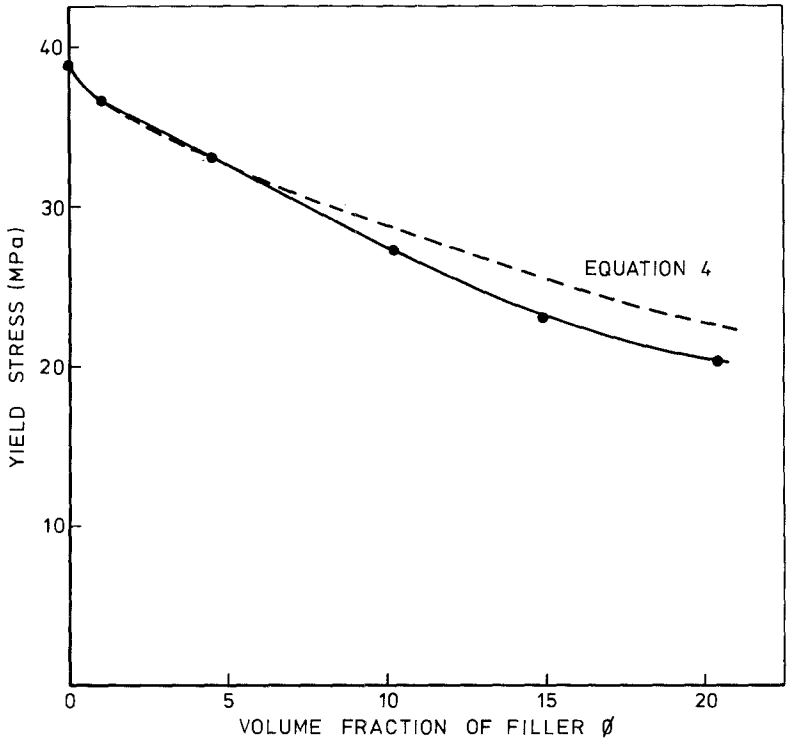

Figure 12 Relationship between yield stress and volume fraction of beads.

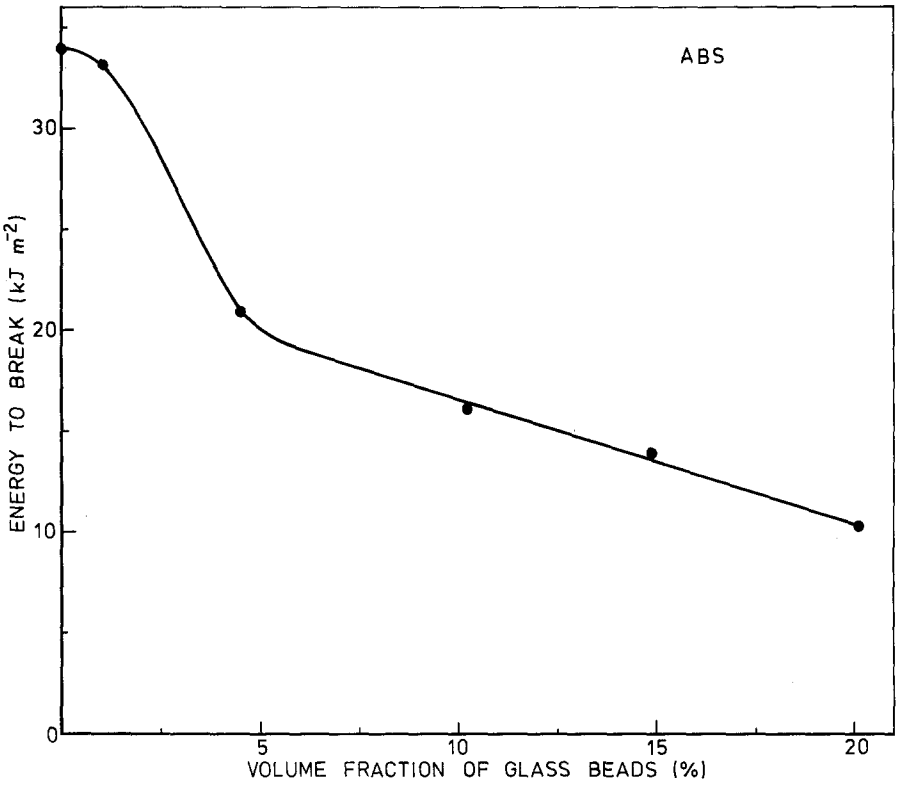

Figure 13 Energy to break in sharp-notch Charpy test at 23° C as a function of bead content.

craze or shear band extends at a later stage of growth, appear to be of greater importance in determining overall creep kinetics. This would explain why the values of γ given in Fig. 9 are all well below 2.0, whereas an elastic stress analysis gives stress concentrations of just over 2.0 for an isolated spherical void [8] and significantly higher values when there is some overlap of stress fields between neighbouring voids or rubber particles [9]. In glass-filled ABS, as in rubber-modified polypropylene [4], it is the average rather than the maximum stress in the region of deformation that is important.

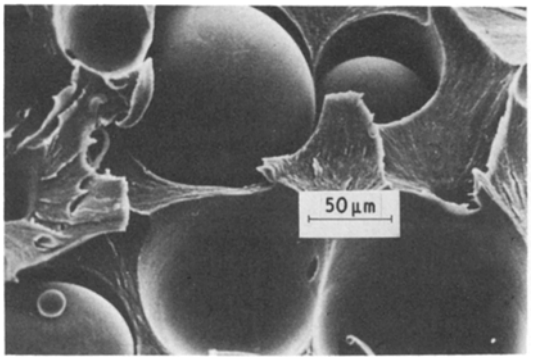

Figure 14 Scanning electron micrograph of fracture surface of ABS material containing 20.4 vol% glass beads subjected to creep test at 15.5 MPa.

Ishai and Cohen's model is surprisingly effective in relating to the volume fraction of voids formed around the glass beads. The model is very simple, since it is based on the reduced load-bearing area of a surface following the path of least resistance through the equators of the voids, and makes no allowance for the known variations in stress concentration within the matrix. Nevertheless it provides a satisfactory approximation for γ that gives some insight into the factors affecting yielding. A rigorous approach requires not only a knowledge of the inhomogenous stress distribution in a material containing a high concentration of randomly dispersed spheres, but also a method for calculating the redistribution of stress following craze or shear band formation, and a deformation criterion that takes account of the tensor nature of stress.

A striking feature of these results is the change in shape of the creep curves with increasing concentration of glass beads. The curves for the unfilled ABS are similar to those obtained previously in experiments on ABS and HIPS: creep is

initially slow, but after a period under load begins to accelerate as a result of multiple craze formation, which is reflected in the volume strain. By contrast, the curves for highly filled ABS show no sign of a slow initial period. Elongation and volume strain increase at a high rate throughout the test. This behaviour which is illustrated in Fig. 4, appears to be associated with the large diameters of the glass microspheres used in this work. Parallel experiments using calcium carbonate particles less than 1 μm diameter blended into the same ABS showed no change in curve shape with filler content. A slow initial period followed by a rapid volume increase was observed in blends containing 20 vol% $CaCO_3$.

The later stages of creep in ABS and its blends with filler particles can be regarded as approximating to a steady state, in which the rate of craze termination is equal to the rate of initiation, so that the overall rate remains constant [6]. If this view is correct, then both the number and size of the crazes or craze packets increases during the initial period until termination becomes effective. Several different mechanisms of termination are probably in operation at the same time, including interaction of growing crazes with large particles (rubber or glass), merging of crazes growing in opposite directions on the same plane, or extension to the edge of the specimen. Any factor that increases the rate of termination relative to the rate of initiation will shorten the intial slow period. The observation that increasing the concentration of glass beads gradually eliminates the slow period is consistent with this conclusion. As the spacing between the beads is reduced, the length to which a craze or set of crazes can grow before meeting an internal surface becomes correspondingly smaller.

In most of the experiments, creep rates increased with time under load, becoming approximately constant at strains greater than about 2.5%, where deformation is due largely to multiple crazing and other dilatational processes. At the highest glass contents, however, creep rates show a decrease with time under load, as illustrated in Fig. 4. A possible explanation of this effect is that the highly stressed material available for conversion to crazes becomes significantly depleted at volume strains of one or two per cent. A simple model to describe this behaviour can be developed on the basis of first-order kinetics, in which the rate of conversion is proportional to the amount of convertible material remaining. If V_{max} is the volume of the material after complete conversion of *available* material to crazes, V_0 is the volume immediately after application of stress, and V_t is the volume after time t under stress, then at constant stress and temperature the rate can be represented by:

$$dV_t/dt = \kappa(V_{max} - V_t)$$

which on integration gives

$$(V_t - V_0)/(V_{max} - V_0) = 1 - \exp(-\kappa t) \quad (5)$$

The volumetric strain data shown in Fig. 4 can be fitted to Equation 5 by assigning a value of 3% to the limiting volume strain $(V_{max} - V_0)$ of the blend containing 20.4 vol% beads. According to this model, only about 3% of the ABS matrix lies within the highly stressed regions defined by the stress concentration factor γ. Increasing the bead content not only increases γ but also accentuates the differences between regions of high stress and the remainder of the material.

From the practical point of view, the effects of the filler particles upon fracture resistance are of greatest interest. In ABS as in SAN [1], rigid filler particles reduce the yield stress, and in that sense behave like rubber particles. Beyond the yield point, however, the two classes of composite behave very differently. Rigid particles cannot match the strains in the surrounding matrix as it crazes or yields, and therefore debond, thus creating an additional stress concentration in the matrix. Rubber particles, on the other hand, are able to deform with the surrounding matrix, provided that there is adequate adhesion between the two components, and thereby actually to lower the stress concentrations in the matrix. Consequently, rigid particles tend to reduce toughness, whereas rubber particles increase it. Nevertheless, there are conditions under which rigid particles can improve fracture resistance, notably when the reduction in yield stress results in a transition from plane strain to plane stress at the crack tip.

In a previous study of filled ABS, Nicolais *et al.* [10] observed an increase in work to break in the tensile test on adding glass beads, essentially because of an increase in elongation to break. In their experiments, stress whitening was very localized in the unfilled ABS, which had an ultimate elongation of only 10%. Addition of glass beads resulted in general whitening along the

length of the test bar, and an increase in elongation to 70 to 80%. No impact data are given, but it is unlikely that the improvement recorded under the special circumstances of the tensile test would be reflected in improved notched impact strength of the filled ABS. Low elongations at break in tension in unfilled ABS appear to be due to shear yielding and incipient neck formation; heavy stress whitening and fracture occur at the neck before yielding has begun in the remainder of the gauge length. Glass beads promote crazing rather than shear yielding, and thus suppress neck formation. These considerations do not apply to three-point bend tests on notched bars.

5. Conclusions

1. Glass beads reinforce ABS at low tensile strains, but debond over a range of strains between 0.1 and 2.0%.

2. Debonding of the beads produces stress concentrations in the surrounding matrix. Average stress concentrations can be predicted approximately by the Ishai–Cohen equation [7].

3. The presence of stress concentrations results in decreases in yield stress and increases in creep rate which can be correlated using the Eyring equation.

4. Changes in the shapes of the creep curves with increasing concentration of glass beads appear to be due to more effective craze termination.

5. The gradual decrease in creep rate with time observed in blends containing 20 vol% glass beads indicates a depletion of the sites available for craze initiation.

6. Debonding of the glass beads from the matrix results in a drastic reduction in fracture resistance as measured in three-point bend tests on notched bars.

References

1. R. E. LAVENGOOD, L. NICOLAIS and M. NARKIS, *J. Appl. Polym. Sci.* **17** (1973) 1173.
2. C. B. BUCKNALL and D. CLAYTON, *J. Mater Sci.* **7** (1972) 202.
3. C. B. BUCKNALL and I. C. DRINKWATER, *ibid.* **8** (1973) 1800.
4. C. B. BUCKNALL and C. J. PAGE, *ibid.* **17** (1982) 808.
5. C. B. BUCKNALL, I. K. PARTRIDGE and M. WARD, *ibid.* **19** (1984) 2064.
6. C. B. BUCKNALL, "Toughened Plastics" (Applied Science, London, 1977) Ch. 7.
7. O. ISHAI and L. J. COHEN, *J. Compos. Mater.* **2** (1968) 302.
8. J. N. GOODIER, *Trans. ASME* **55** (1933) 39.
9. L. J. BROUTMAN and G. PANIZZA, *Int. J. Polym. Mater.* **1** (1971) 95.
10. L. NICOLAIS, E. DRIOLI and R. F. LANDEL, *Polymer* **14** (1973) 21.

Received 21 June
and accepted 6 July 1984